Supporting Information

Ni_5P_4-NiP_2-Ni_2P Nanocomposites Tangled with N-Doped Carbon for Enhanced Electrochemical Hydrogen Evolution in Acidic and Alkaline Solutions

Miaomiao Pei [1], Xiaowei Song [1,2,*], Haihong Zhong [2,3,*], Luis A. Estudillo-Wong [4], Yingchun Gao [1], Tongmengyao Jin [1], Ju Huang [1], Yali Wang [1], Jun Yang [5] and Yongjun Feng [2,*]

1 Key Laboratory of Functional Coordination Compounds of Anhui Higher Education Institutes, School of Chemistry and Chemical Engineering, Anqing Normal University, Anqing 246011, China
2 State Key Laboratory of Chemical Resource Engineering, Beijing Engineering Center for Hierarchical Catalysts, College of Chemistry, Beijing University of Chemical Technology, No. 15 Beisanhuan East Road, Beijing 100029, China
3 College of Science, Hainan University, Haikou 570228, China
4 Departamento de Biociencias e Ingeniería, CIIEMAD-IPN, Instituto Politécnico Nacional, Calle 30 de junio de 1520, Alcaldía GAM, C.P. 07340, Ciudad de México, México
5 State Key Laboratory of Multiphase Complex Systems, Institute of Process Engineering, Chinese Academy of Sciences, Beijing 100190, China.

* Correspondence: songxw@aqnu.edu.cn (X. S.); hzhong@buct.edu.cn (H. Z.); yjfeng@mail.buct.edu.cn (Y. F.)

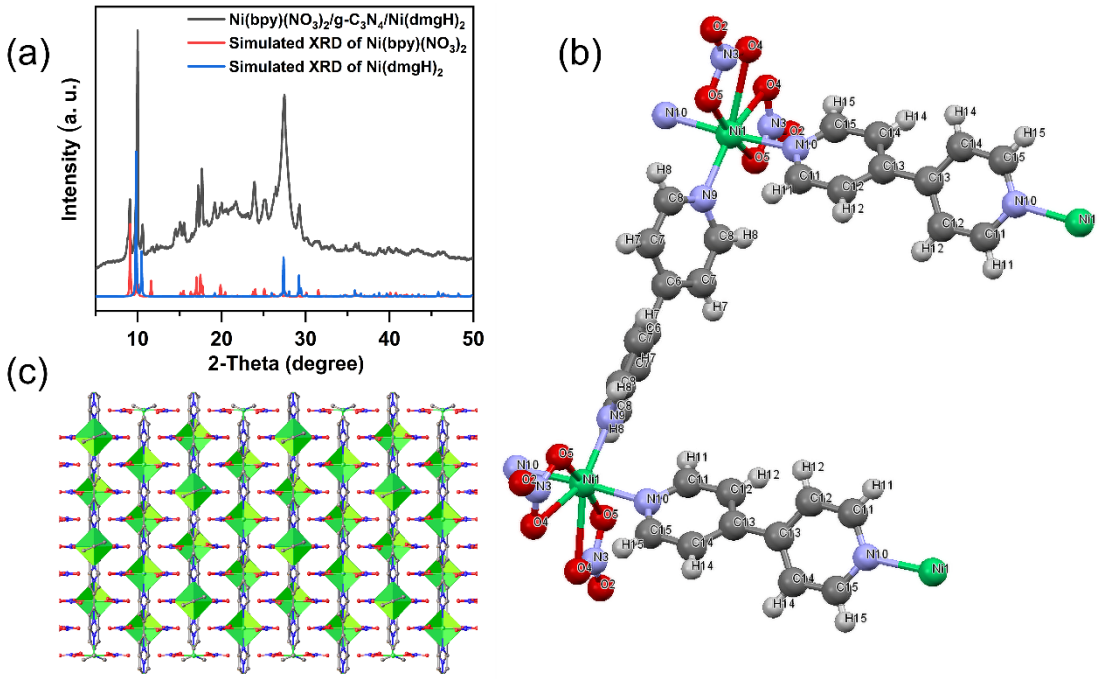

Figure S1 (a) XRD pattern of the precursor $Ni(bpy)(NO_3)_2/g\text{-}C_3N_4/Ni(dmgH)_2$ and simulated XRD patterns of $Ni(bpy)(NO_3)_2$ and $Ni(dmgH)_2$, (b) and (c) the crystal structure of $Ni(bpy)(NO_3)_2$. (The compound $Ni(bpy)(NO_3)_2$ crystallizes in the orthorhombic space group *Fddd*, a = 11.2717(3) *Å*, b= 20.6009(8) *Å*, c = 34.4255(11) *Å*, $\alpha = \beta = \gamma = 90°$, V = 7993.8(5) $Å^3$, R_1 / wR_2 ($I > 2\sigma(I)$) = 0.0498/0.1443, R_1 / wR_2 (all data) = 0.0588/0.1542, GooF = 1.056; the simulated XRD patterns of $Ni(bpy)(NO_3)_2$ and $Ni(dmgH)_2$ originated from the single crystal data, while the single crystal file of $Ni(dmgH)_2$ was obtained from the CCDC No.759570)

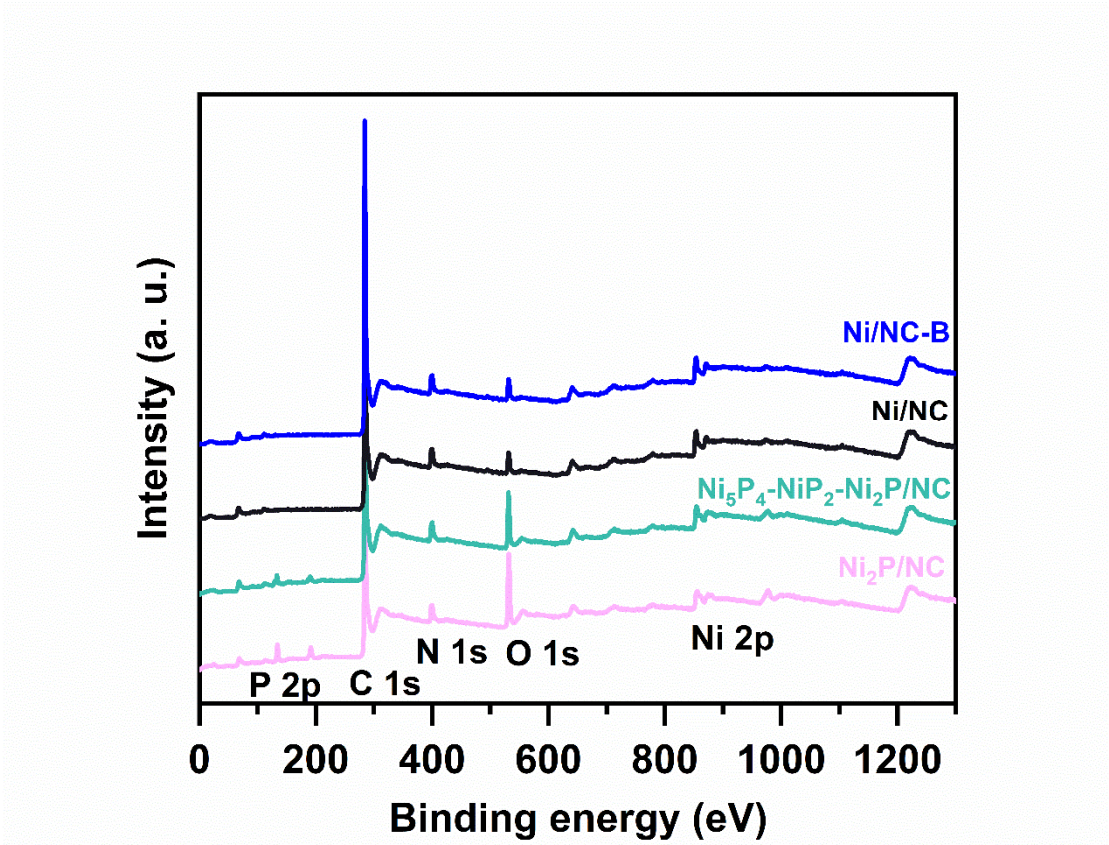

Figure S2 X-ray photoelectron spectra of Ni/NC, Ni_2P/NC, Ni_5P_4-NiP_2-Ni_2P/NC and Ni/NC-B

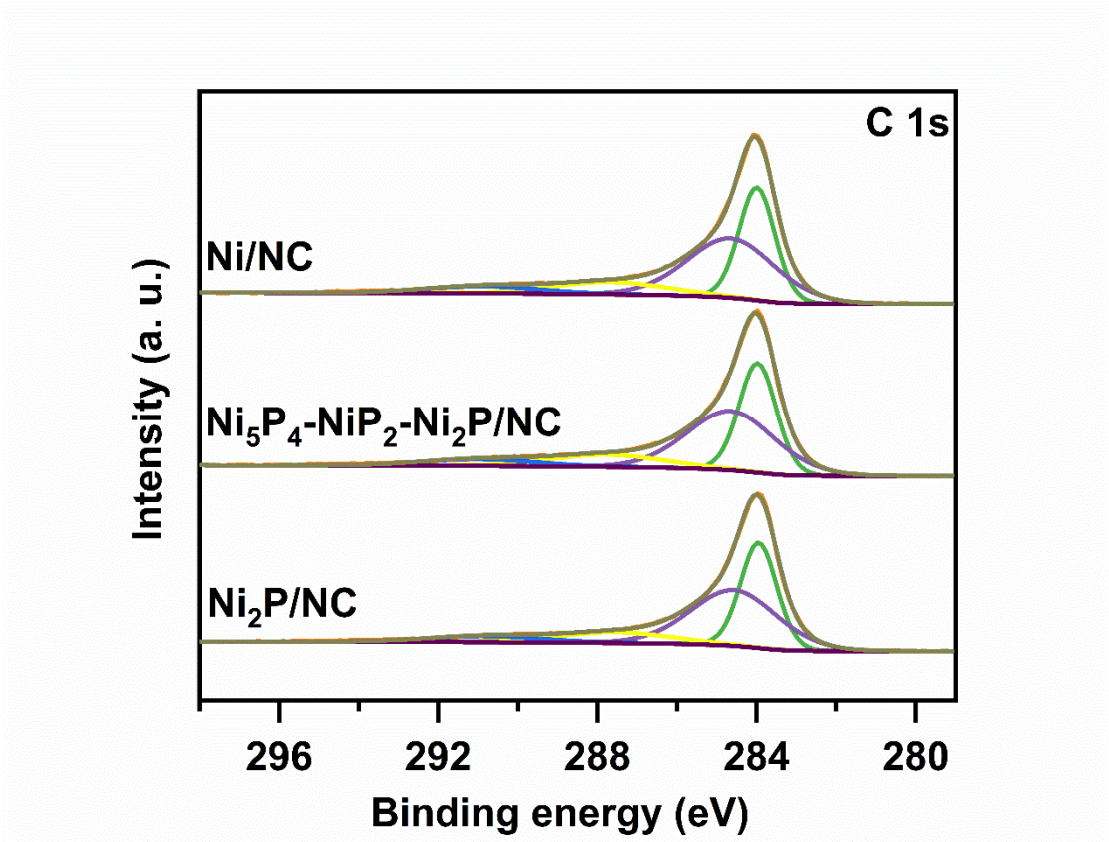

Figure S3 High-resolution XPS spectra of C 1s for the samples Ni/NC, Ni_2P/NC and Ni_5P_4-NiP_2-Ni_2P/NC

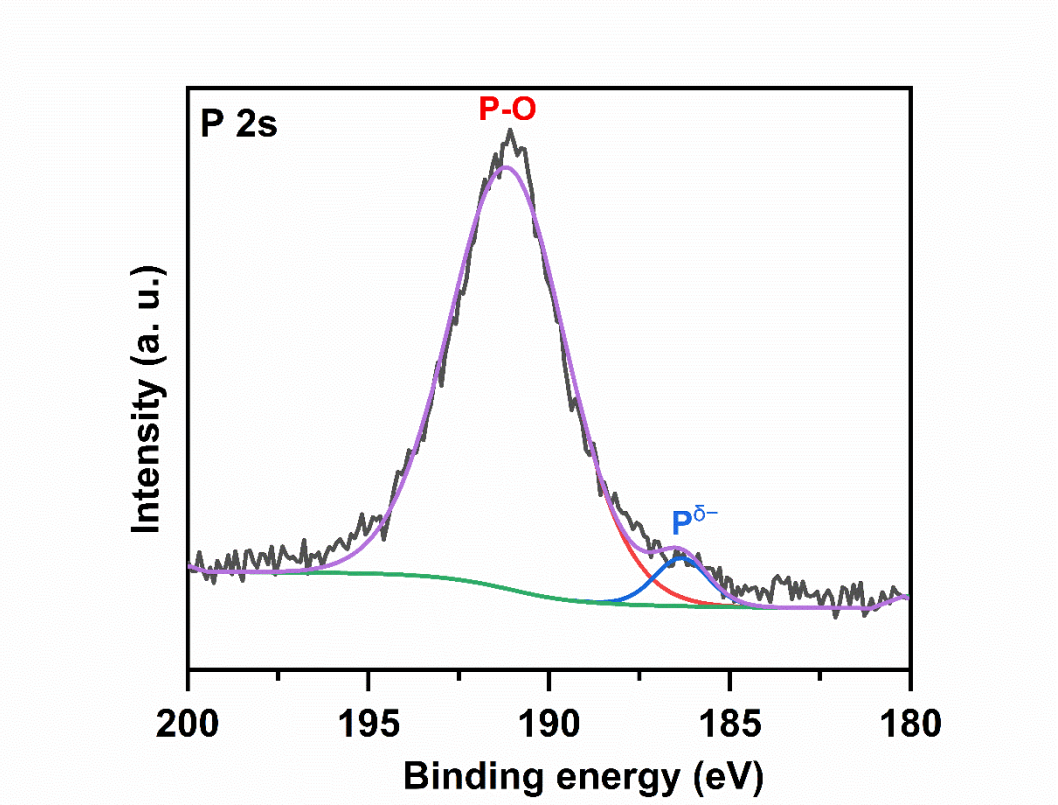

Figure S4 High-resolution XPS spectrum of P 2s for the sample Ni_2P/NC

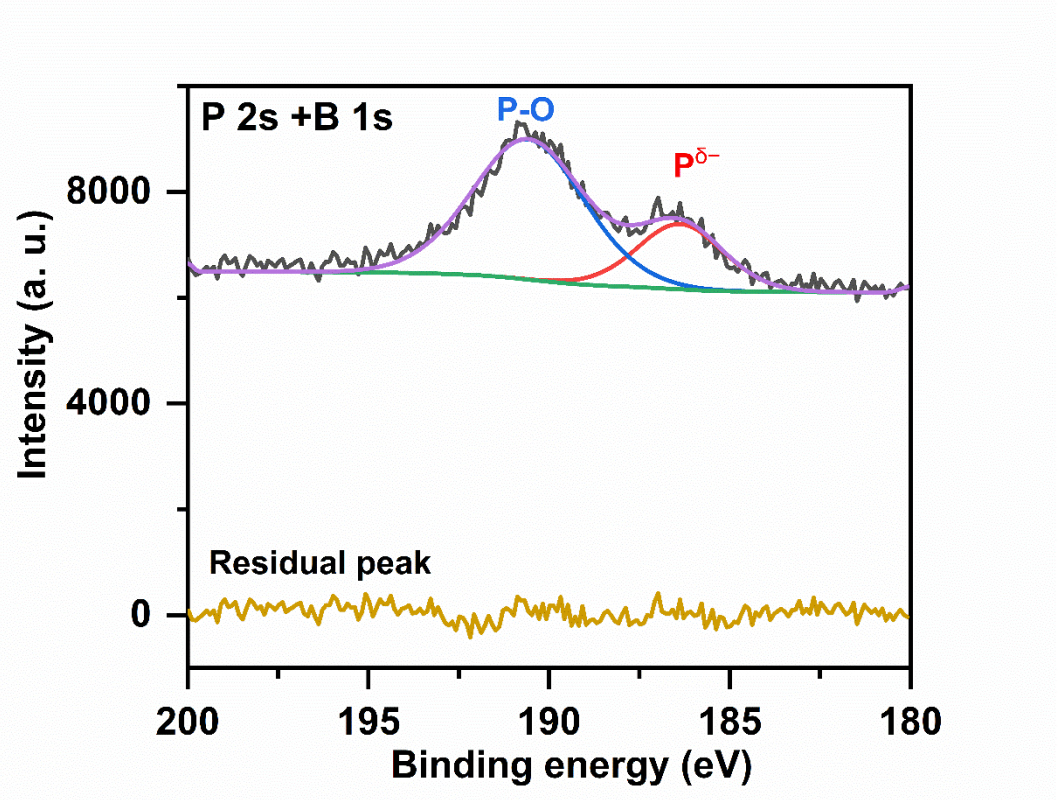

Figure S5 High-resolution XPS spectra of P 2s +B 1s for the sample Ni_5P_4-NiP_2-Ni_2P/NC

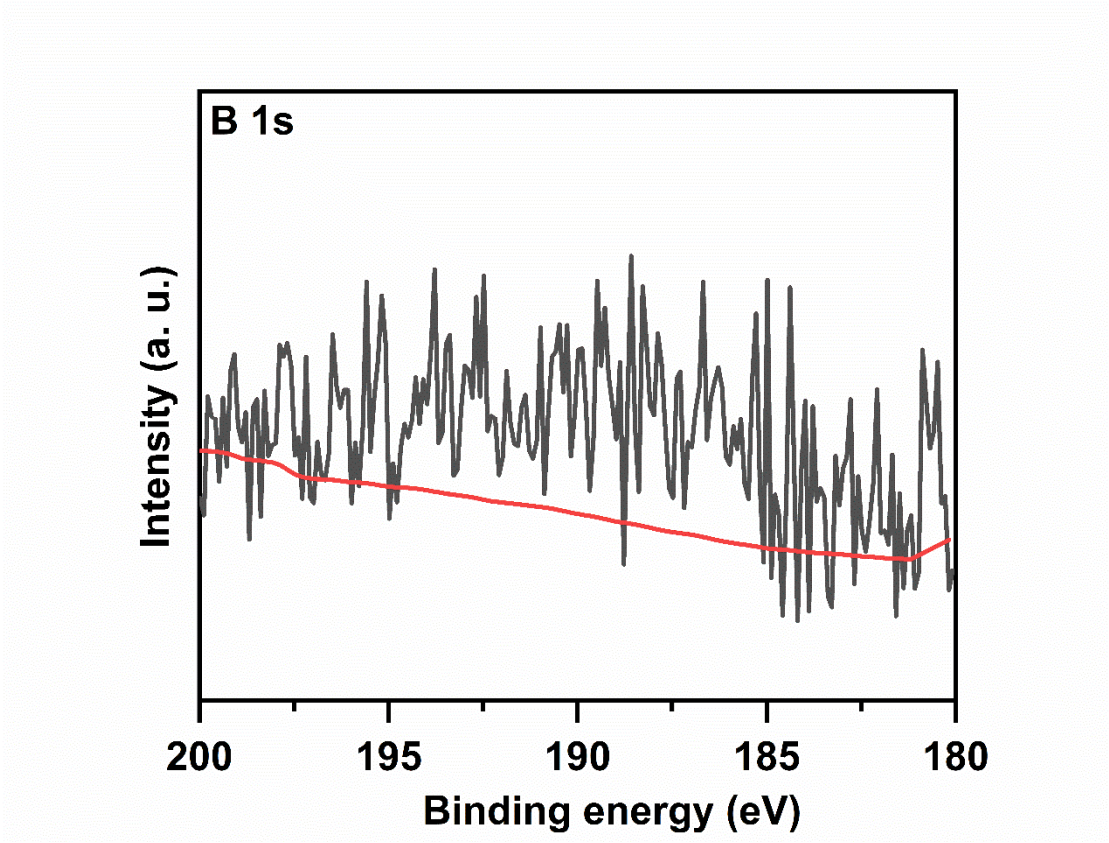

Figure S6 High-resolution XPS spectrum of B 1s for the sample Ni/NC-B

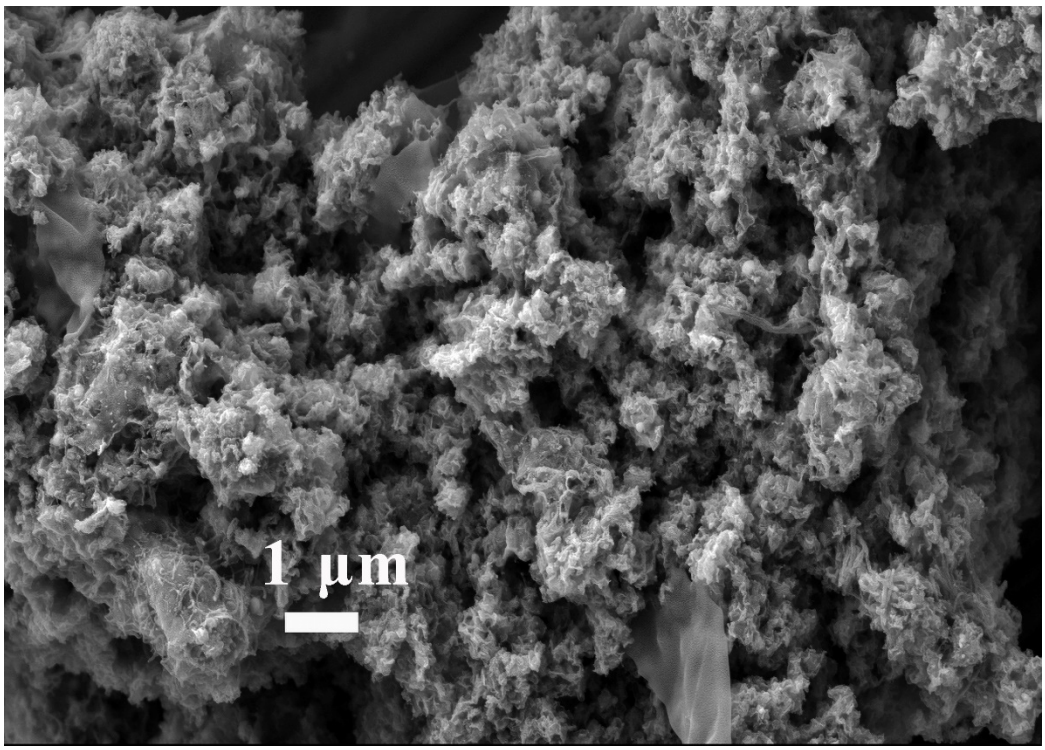

Figure S7 SEM image for Ni_5P_4-NiP_2-Ni_2P/NC after the chronopotentiometric test in 0.5 M H_2SO_4 solution

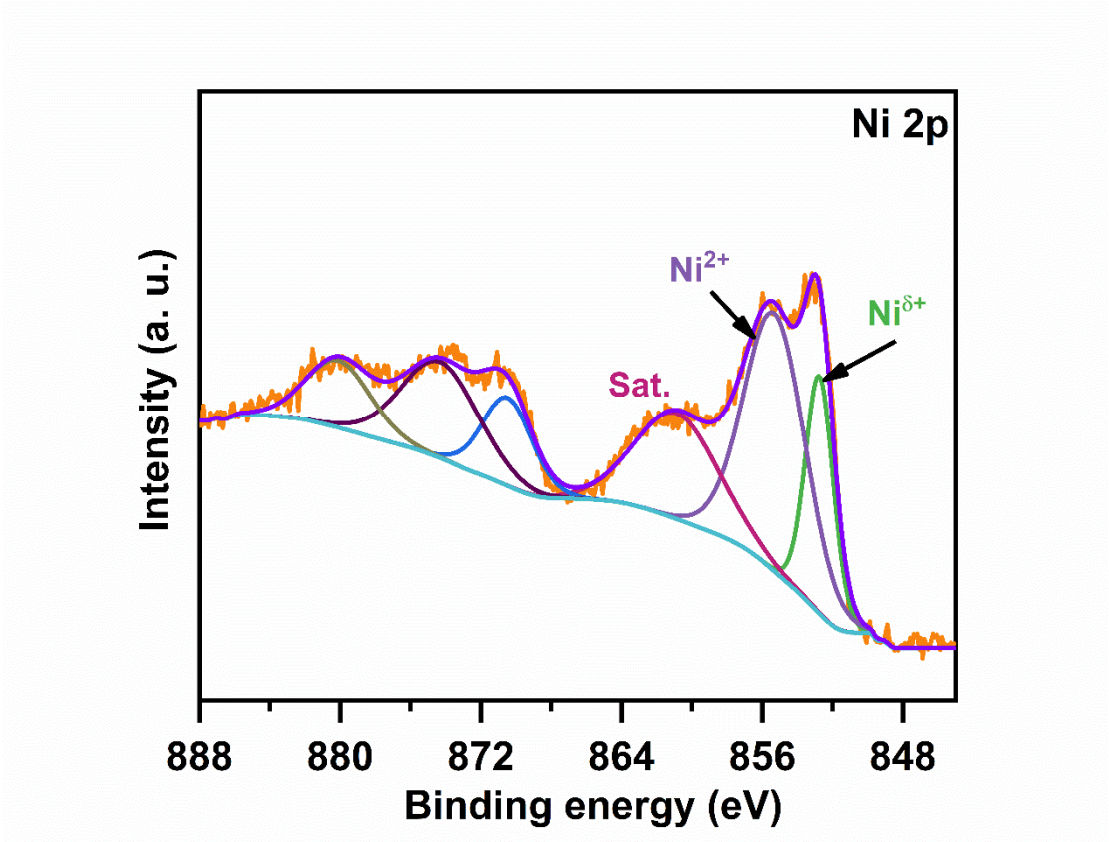

Figure S8 XPS high-resolution spectrum of Ni 2p for Ni_5P_4-NiP_2-Ni_2P/NC after the chronopotentiometric test in 0.5 M H_2SO_4 solution

.

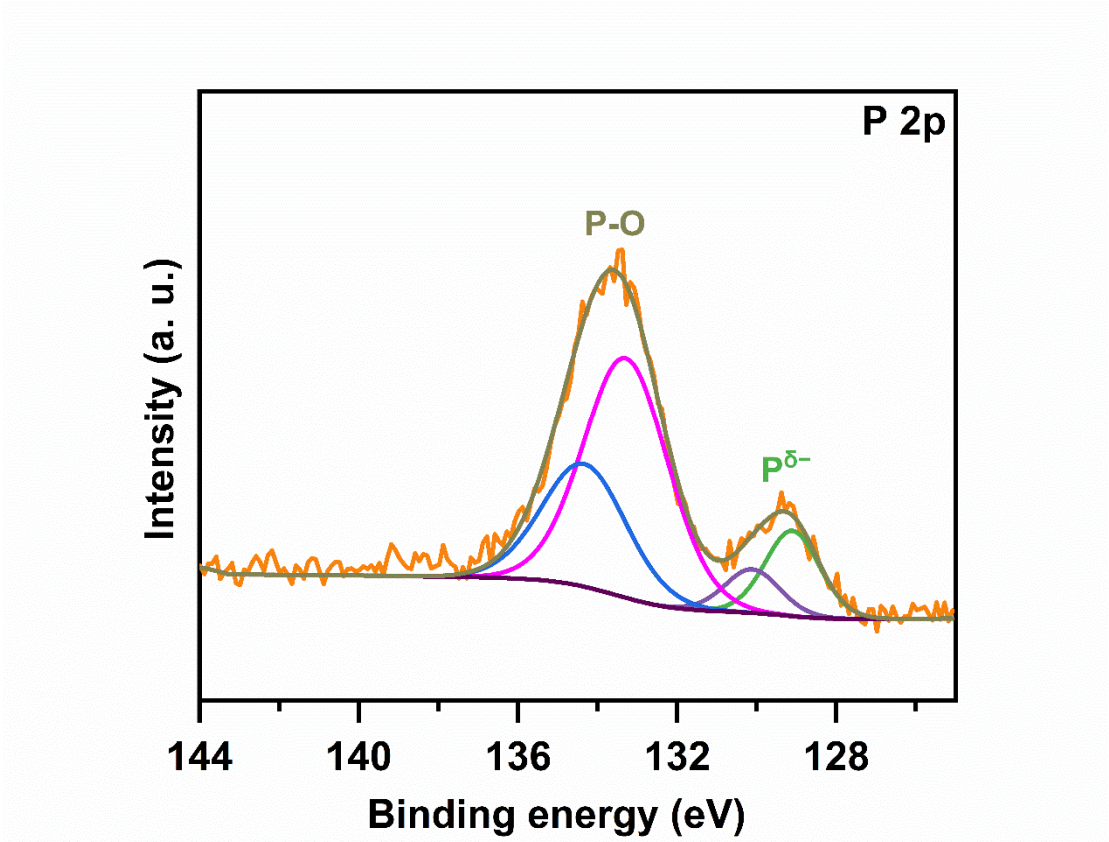

Figure S9 XPS high-resolution spectrum of P 2p for Ni_5P_4-NiP_2-Ni_2P/NC after the chronopotentiometric test in 0.5 M H_2SO_4 solution

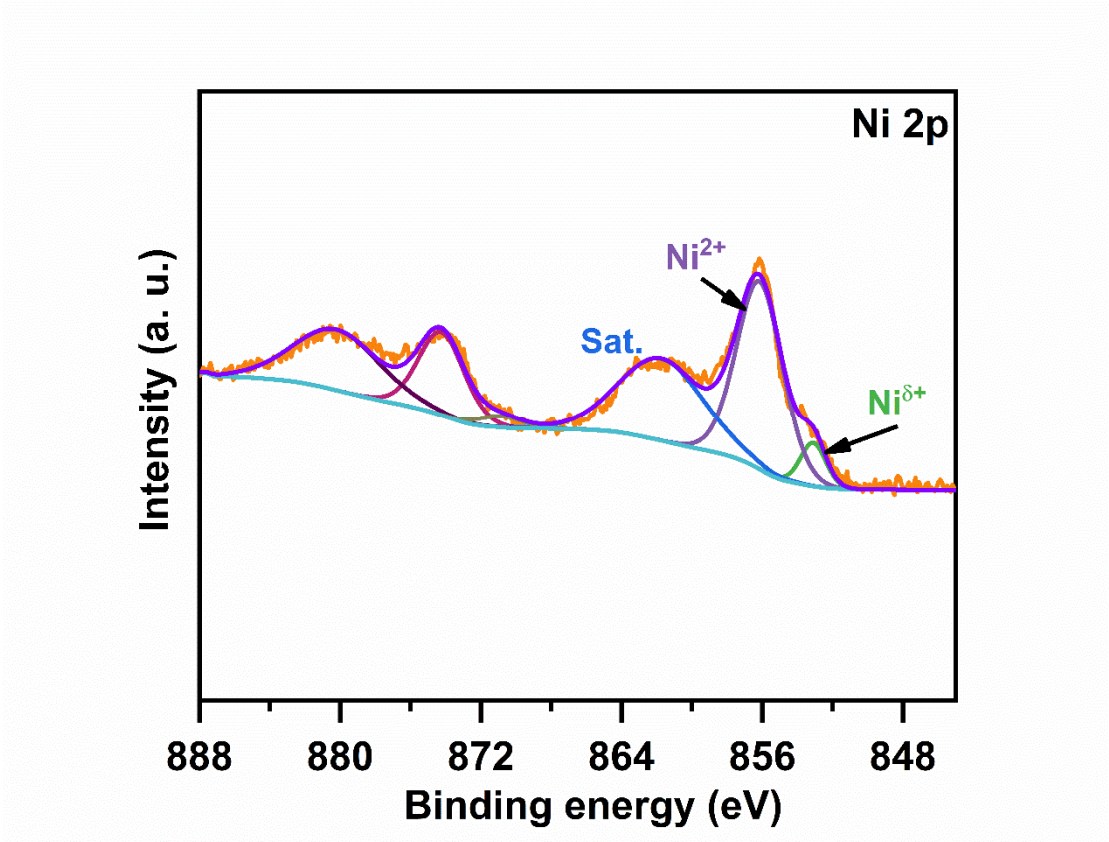

Figure S10 XPS high-resolution spectrum of Ni 2p for Ni_5P_4-NiP_2-Ni_2P/NC after the chronopotentiometric test in 1 M KOH solution

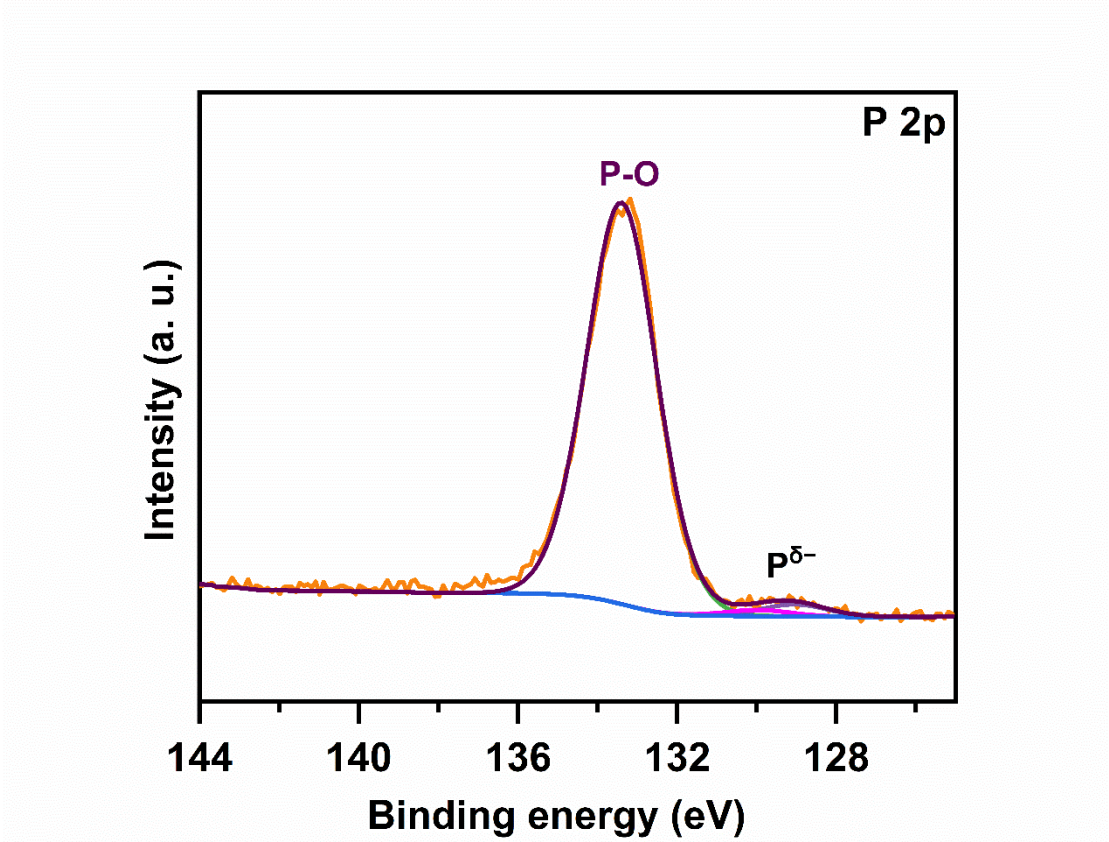

Figure S11 XPS high-resolution spectrum of P 2p for Ni_5P_4-NiP_2-Ni_2P/NC after the chronopotentiometric test in 1 M KOH solution

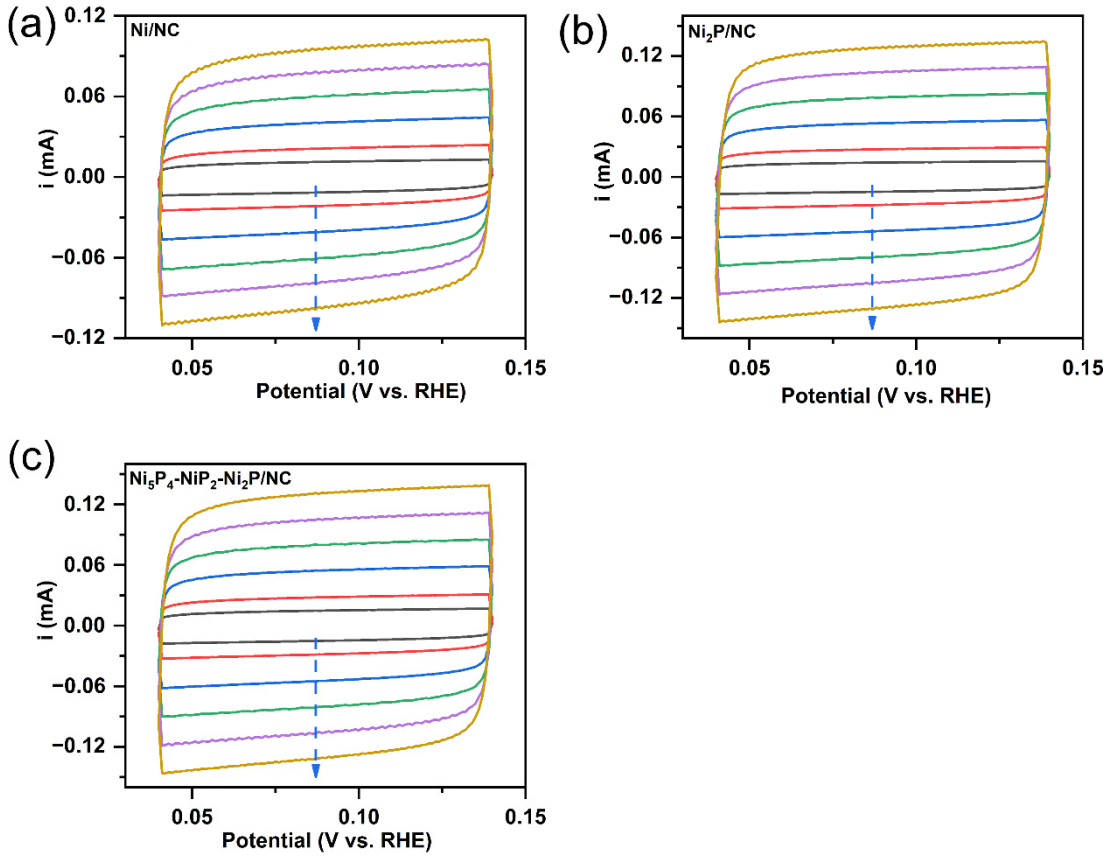

Figure S12 Electrochemical double-layer capacitance (C_{dl}) measurements in 0.5 M H_2SO_4 for (a) Ni/NC, (b) Ni_2P/NC, and (c) Ni_5P_4-NiP_2-Ni_2P/NC using CV scans at different scan rates from 10 to 100 $mV \cdot s^{-1}$

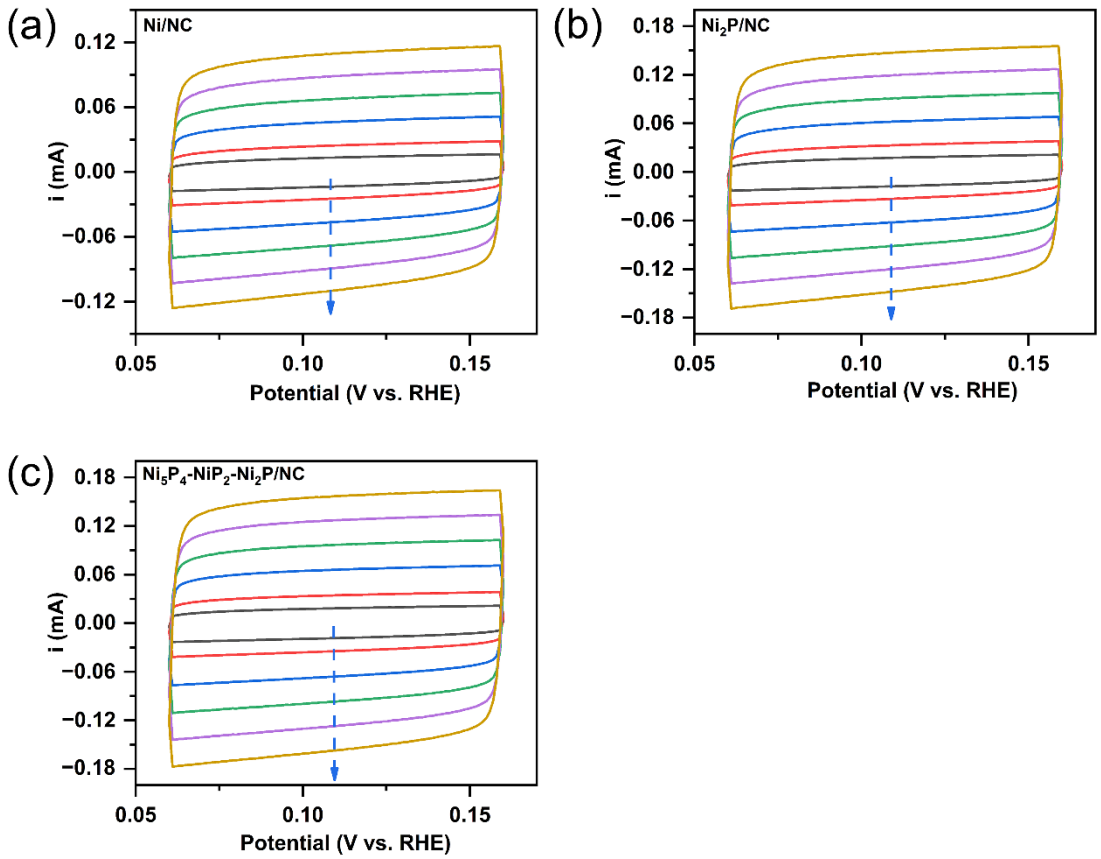

Figure S13 Electrochemical double-layer capacitance (C_{dl}) measurements in 1 M KOH for (a) Ni/NC, (b) Ni_2P/NC, and (c) Ni_5P_4-NiP_2-Ni_2P/NC using CV scans at different scan rates from 10 to 100 $mV \cdot s^{-1}$

Table S1 Microstructural properties obtained by RRM for the sample Ni_5P_4-NiP_2-Ni_2P/NC

Phases	Mass percentage wt.%	Lattice parameter Å	Crystallite size nm
Ni_5P_4 ($P6_3mc$)	35.84 (0.48)	a = b = 6.7909 (5×10^{-4}) c = 10.9954 (1×10^{-3})	90.4 (3.4)
NiP_2 ($Pa\bar{3}$)	49.26 (0.66)	a = 5.4547 (3×10^{-4})	70.6 (1.3)
Ni_2P ($P\bar{6}2m$)	14.90 (0.42)	a = b = 5.8744 (2×10^{-3}) c = 3.3858 (2×10^{-3})	30.3 (1.3)

Table S2 Surface atomic compositions obtained from XPS spectra for the as-prepared samples

samples	C 1s (at %)	O 1s (at %)	N 1s (at %)	P 2p (at %)	Ni 2p (at %)
Ni_2P/NC	80.57	11.01	5.25	1.85	1.32
Ni_5P_4-NiP_2-Ni_2P/NC	83.16	6.99	5.77	2.62	1.46
Ni/NC	89.21	3.56	6.00	0	1.24

Table S3 Comparison of the HER performance of the heterostructured catalysts comprising different nickel phosphides in the literatures and this work

Catalysts	Substrate [a]	0.5 M H_2SO_4			1 M KOH			Refs
		η_{10} (mV)	Tafel slope (mV dec^{-1})	Loading (mg cm^{-2})	η_{10} (mV)	Tafel slope (mV dec^{-1})	Loading (mg cm^{-2})	
Ni_5P_4-NiP_2-Ni_2P/NC	GCE	168	69	0.204	202	74	0.204	This work
Ni_2P/Ni_5P_4@NC-30	GCE	104	38.5	0.35	113	89.5	0.35	[1]
Ni_2P@PCG	GCE	110	58.6	0.51	150	79.4	0.51	[2]
Ni_2P/CNS	GCE	174	64	0.429	315	120	0.429	[3]
Ni_2P@C-400	GCE	186	64	0.566	342	N/A	0.566	[4]
Ni_2P/CNT	GCE	124	53	0.184	N/A	N/A	N/A	[5]
Ni_2P/Ni_5P_4@3DNG	GCE	139	59	N/A	N/A	N/A	N/A	[6]
Ni_2P-MOF	GCE	172	62	0.35	N/A	N/A	N/A	[7]
Ni_2P/C	GCE	198	113.2	N/A	N/A	N/A	N/A	[8]

Ni-$Ni_{12}P_5$@CNTs/ rGO-0.5	GCE	217.4	69.33	0.102	N/A	N/A	N/A	[9]
$Ni_{12}P_5$-Ni_2P/Ni/NF	Ni/NF	83	68	N/A	129	70	N/A	[10]
Ni_5P_4-Ni_2P-NS	NF	120	79.1	N/A	N/A	N/A	N/A	[11]
Ni_2P-NRs/Ni	NF	131	106.1	N/A	N/A	N/A	N/A	[12]
Ni_5P_4-NiP_2 nanosheet	NF	174	83.9	N/A	N/A	N/A	N/A	[13]
Ni_2P–NiP_2 hollow nanoparticle	NF	N/A	N/A	N/A	59.7	58.8	5	[14]
Ni_2P–$Ni_{12}P_5$/NF	NF	N/A	N/A	N/A	76	68	N/A	[15]
Ni_2P@NC/NF	NF	N/A	N/A	N/A	93	77.83	N/A	[16]
Ni_2P/CC	CC	119	50	N/A	148	N/A	N/A	[17]
NiP_2-650(c/m)	CC	160	60.2	N/A	134	67	N/A	[18]

CC@Ni-P	CC	93	58.2	N/A	N/A	N/A	N/A	[19]
$Ni_{12}P_5$-Ni_2P	CC	166	60	0.25	N/A	N/A	N/A	[20]
Ni_2P-Ni_5P_4 arrays	CC	N/A	N/A	N/A	102	83	N/A	[21]

[a] GCE: glassy carbon electrode, NF: nickel foam, CC: carbon cloth; N/A: Not available

Table S4 Electrochemical active surface area (ECSA) of the as-prepared composites

Catalysts	Electrolytes	C_{dl} (μF)	ECSA (cm^2)
Ni_2P/NC	0.5 M H_2SO_4	1300	32.5
	1 M KOH	1500	37.5
Ni_5P_4-NiP_2-Ni_2P/NC	0.5 M H_2SO_4	1320	33
	1 M KOH	1590	39.8
Ni/NC	0.5 M H_2SO_4	980	24.5
	1 M KOH	1110	27.8

References

1. Hong, W.; Lv, C.; Sun, S.; Chen, G. Fabrication and Study of the Synergistic Effect of Janus Ni_2P/Ni_5P_4 Embedded in N-Doped Carbon as Efficient Electrocatalysts for Hydrogen Evolution Reaction. *Catal. Sci. Technol.* **2020**, *10*, 1023-1029.

2. Miao, M.; Hou, R.; Liang, Z.; Qi, R.; He, T.; Yan, Y.; Qi, K.; Liu, H.; Feng, G.; Xia, B.Y. Chainmail Catalyst of Ultrathin P-Doped Carbon Shell-Encapsulated Nickel Phosphides on Graphene towards Robust and Efficient Hydrogen Generation. *J. Mater. Chem. A* **2018**, *6*, 24107-24113.

3. Li, Y.; Cai, P.; Ci, S.; Wen, Z. Strongly Coupled 3D Nanohybrids with Ni_2P/Carbon Nanosheets as pH-Universal Hydrogen Evolution Reaction Electrocatalysts. *ChemElectroChem* **2017**, *4*, 340-344.

4. He, S.; He, S.; Gao, F.; Bo, X.; Wang, Q.; Chen, X.; Duan, J.; Zhao, C. Ni_2P@carbon Core-Shell Nanorod Array Derived from ZIF-67-Ni: Effect of Phosphorization Temperature on Morphology, Structure and Hydrogen Evolution Reaction Performance. *Appl. Surf. Sci.* **2018**, *457*, 933-941.

5. Pan, Y.; Hu, W.; Liu, D.; Liu, Y.; Liu, C. Carbon Nanotubes Decorated with Nickel Phosphide Nanoparticles as Efficient Nanohybrid Electrocatalysts for the Hydrogen Evolution Reaction. *J. Mater. Chem. A* **2015**, *3*, 13087-13094.

6. Ding, G.; Zhang, Y.; Dong, J.; Xu, L. Fabrication of Ni_2P/Ni_5P_4 Nanoparticles Embedded in Three-Dimensional N-Doped Graphene for Acidic Hydrogen Evolution Reaction. *Mater. Lett.* **2021**, *299*, 130071.

7. Tian, T.; Ai, L.; Jiang, J. Metal–Organic Framework-Derived Nickel Phosphides as Efficient Electrocatalysts toward Sustainable Hydrogen Generation from Water Splitting. *RSC Adv.* **2015**, *5*, 10290-10295.

8. He, S.; He, S.; Bo, X.; Wang, Q.; Zhan, F.; Wang, Q.; Zhao, C. Porous Ni_2P/C Microrods Derived from Microwave-Prepared MOF-74-Ni and Its Electrocatalysis for Hydrogen Evolution Reaction. *Mater. Lett.* **2018**, *231*, 94-97.

9. Chen, L.; Wu, P.; Yang, S.; Qian, K.; Sun, W.; Wei, W.; Xu, Y.; Xie, J. Fabrication of CNTs Encapsulated Nickel-Nickel Phosphide Nanoparticles on Graphene for Remarkable Hydrogen Evolution Reaction Performance. *J. Electroanal. Chem.* **2019**, *846*, 113142.

10. Zhang, J.; Zhang, Z.; Ji, Y.; Yang, J.; Fan, K.; Ma, X.; Wang, C.; Shu, R.; Chen, Y. Surface Engineering Induced Hierarchical Porous $Ni_{12}P_5$-Ni_2P Polymorphs Catalyst for Efficient Wide pH Hydrogen Production. *Appl. Catal. B: Environ.* **2021**, *282*, 119609.

11. Wang, X.; Kolen'ko, Y.V.; Bao, X.-Q.; Kovnir, K.; Liu, L. One-Step Synthesis of Self-Supported Nickel Phosphide Nanosheet Array Cathodes for Efficient Electrocatalytic Hydrogen Generation. *Angew. Chem. Int. Ed.* **2015**, *54*, 8188-8192.

12. Wang, X.; Kolen'ko, Y.V.; Liu, L. Direct Solvothermal Phosphorization of Nickel Foam to Fabricate Integrated Ni_2P-Nanorods/Ni Electrodes for Efficient Electrocatalytic Hydrogen Evolution. *Chem. Commun.* **2015**, *51*, 6738-6741.

13. Cai, W.; Liu, W.; Sun, H.; Li, J.; Yang, L.; Liu, M.; Zhao, S.; Wang, A. Ni_5P_4-NiP_2 Nanosheet Matrix Enhances Electron-Transfer Kinetics for Hydrogen Recovery in Microbial Electrolysis Cells. *Appl. Energ*. **2018**, *209*, 56-64.

14. Liu, T.; Li, A.; Wang, C.; Zhou, W.; Liu, S.; Guo, L. Interfacial Electron Transfer of Ni_2P–NiP_2 Polymorphs Inducing Enhanced Electrochemical Properties. *Adv. Mater.* **2018**, *30*, 1803590.
15. Wang, Z.; Wang, S.; Ma, L.; Guo, Y.; Sun, J.; Zhang, N.; Jiang, R. Water-Induced Formation of Ni_2P–$Ni_{12}P_5$ Interfaces with Superior Electrocatalytic Activity toward Hydrogen Evolution Reaction. *Small* **2021**, *17*, 2006770.
16. Zhang, H.; Li, W.; Feng, X.; Zhu, L.; Fang, Q.; Li, S.; Wang, L.; Li, Z.; Kou, Z. A Chainmail Effect of Ultrathin N-Doped Carbon Shell on Ni_2P Nanorod Arrays for Efficient Hydrogen Evolution Reaction Catalysis. *J. Colloid Interf. Sci.* **2022**, *607*, 281-289.
17. Huo, S.; Yang, S.; Niu, Q.; Yang, F.; Song, L. Synthesis of Functional Ni_2P/CC Catalyst and the Robust Performances in Hydrogen Evolution Reaction and Nitrate Reduction. *Int. J. Hydrogen Energ.* **2020**, *45*, 4015-4025.
18. Fu, Q.; Wang, X.; Han, J.; Zhong, J.; Zhang, T.; Yao, T.; Xu, C.; Gao, T.; Xi, S.; Liang, C.; Xu, L.; Xu, P.; Song, B. Phase-Junction Electrocatalysts towards Enhanced Hydrogen Evolution Reaction in Alkaline Media. *Angew. Chem. Int. Ed.* **2021**, *60*, 259-267.
19. Chen, A.; Fu, L.; Xiang, W.; Wei, W.; Liu, D.; Liu, C. Facile Synthesis of Ni_5P_4 Nanosheets/Nanoparticles for Highly Active and Durable Hydrogen Evolution. *Int. J. Hydrogen Energ.* **2021**, *46*, 11701-11710.
20. Shi, H.; Yu, Q.; Liu, G.; Hu, X. Promoted Electrocatalytic Hydrogen Evolution Performance by Constructing $Ni_{12}P_5$–Ni_2P Heterointerfaces. *Int. J. Hydrogen Energ.* **2021**, *46*, 17097-17105.
21. Yan, Y.; Lin, J.; Bao, K.; Xu, T.; Qi, J.; Cao, J.; Zhong, Z.; Fei, W.; Feng, J. Free-Standing Porous Ni_2P-Ni_5P_4 Heterostructured Arrays for Efficient Electrocatalytic Water Splitting. *J. Colloid Interf. Sci.* **2019**, *552*, 332-336.